Zero-field level crossing and optical radio-frequency double resonance studies of the A $^2\Sigma^+$ states of OH and OD

K. R. German *, T. H. Bergeman[†], E. M. Weinstock[‡], and R. N. Zare

Department of Chemistry, Columbia University, New York, New York 10027

(Received 27 July 1972)

We have performed Hanle effect and double resonance measurements on the $v'=0$, $N'=2$, $J'=3/2$ level of the OH A $^2\Sigma^+$ state and on the $v'=0$, $N'=1$, $J'=3/2$ level of the OD A $^2\Sigma^+$ state using atomic line excitation. The double resonance signal is followed as a function of static magnetic field. For OH the Zeeman splitting is found to be linear up to the highest fields investigated whereas in OD the deviations from linearity yield a value for the combination of hyperfine constants $b+c/5=121\pm14$ MHz. In the case of OH, both the $F'=1$ and $F'=2$ hyperfine components contribute to the Hanle signal; in the case of OD, the Hanle signal arises almost entirely from the $F'=5/2$ component. In the former case, measurement of the relative intensities of the $F'=1$ and $F'=2$ double resonance signals gives the relative populations of these components. From the linewidths of the zero-field level crossings, along with the analysis of the optical double resonance data, the radiative lifetimes for the above (v',N',J') levels of the A $^2\Sigma^+$ states of OH and OD are determined to be 0.58 ± 0.05 and 0.65 ± 0.05 μsec, respectively.

I. INTRODUCTION

Because of its wide occurrence, the OH diatomic molecule is of considerable importance. It is observed in such diverse environments as emission in flames, airglow in the upper atmosphere, and maser action in the interstellar medium. In addition, since OH is a first-row diatomic hydride, a comparison of its experimental properties with quantum calculations is apt to be more meaningful than an equivalent comparison with heavier systems. The two lowest electronic states, X $^2\Pi$ and A $^2\Sigma^+$, are responsible for the OH ultraviolet band system that has been extensively studied spectroscopically by Dieke and Crosswhite.[1] In addition, the hyperfine structure of the X $^2\Pi$ state was first measured in the pioneering experiments of Dousmanis, Sanders, and Townes,[2] and has been extensively studied since.[3] There are, however, no such corresponding hyperfine measurements for the A state because of its short lifetime.

Optical radio-frequency double-resonance measurements reported for the A $^2\Sigma^+$ states of OH[4,5] and of OD[6] have exhibited a linear Zeeman effect for resonance frequencies equal to or lower than 15 MHz for OH and 5 MHz for OD. For the corresponding field strengths, the angular momentum coupling scheme of the molecular excited state obeys Hund's case $(b_{\beta J})$ to within experimental error. By combining g-value measurements with the level-crossing studies, radiative lifetimes have been obtained.[4–6] However, in the case of OH previous studies have not correctly accounted for the relative contributions of the excited state hyperfine components to the Hanle signal.

We report here double-resonance studies in the intermediate-field region for the OD molecule. By applying the theory of double resonance, we are able to assign the observed double resonance signal at intermediate field to a transition between a single pair of (F, M_F) sublevels. The OD double resonance

frequencies deviate from linearity as a function of magnetic field. This permits an initial determination of the hyperfine splitting for the A state of OD, and hence the positions of high-field level crossings.[7] Refinements in the zero-field level crossing measurements over our previous work combined with a more detailed consideration of the relative contributions of the various hyperfine levels to the Hanle signal also lead to an improved value for the radiative lifetime of the (v', N', J') levels studied in the A states of OH and OD. Some evidence of other workers is presented to show that the radiative lifetime for a given vibrational level v varies with N and J. This variation of the radiative lifetime with rotational level helps to reconcile the differences between other recent lifetime determinations.

II. EXPERIMENTAL

The OH and OD radicals are generated by the chemical reactions[8]

$$H + NO_2 \rightarrow OH + NO$$

and

$$D + NO_2 \rightarrow OD + NO$$
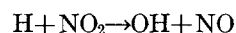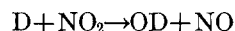
in a flow system described previously.[4] A block diagram of the experimental setup is presented in Fig. 1. This apparatus differs from that used earlier in the use of a single photomultiplier to observe the perpendicular fluorescence and through the addition of a PDP LAB/8 signal averager. In the case of OH, the lamp is an electrodeless microwave discharge in Zn vapor whose 3072.06-Å line excites the $v=0$, $N=2$, $J=3/2$ level of the OH A $^2\Sigma^+$ state through the coincidence of the R_{21} (1) absorption line.[9] For the OD molecule, we use a microwave-excited barium flow lamp whose 3071.60-Å line excites the $v=0$, $N=1$, $J=3/2$ level of the A state through the coincidence with the $Q_1(1)$ absorption line.[10] The pressure-measuring devices are

FIG. 1. Block diagram of apparatus. Not shown are (1) pairs of Helmholtz coils used to null the local magnetic field and to modulate the static magnetic field, and (2) linear polarizers and rf coils used in the double-resonance measurements.
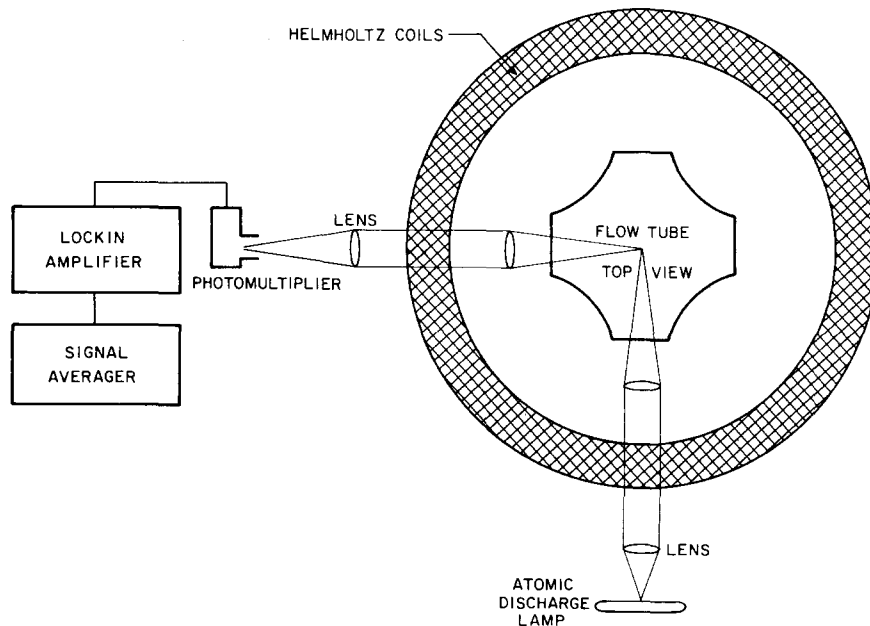
the same as used before. In the present studies, however, the well-known Hg $6\,{}^3P_1$–$6\,{}^1S_0$ double-resonance signal[12] is used to calibrate the static magnetic field to an accuracy of 0.1%. Throughout this paper, all experimental errors represent three standard deviations.

A. Double Resonance Measurements

For the double resonance studies, the tendency of the electric rf field to cause gaseous discharge in the flow tube restricts the rf magnetic fields that can be obtained to about 0.5 G and provides the fundamental limitation on the extension of these measurements to higher frequencies. It is found that an rf coil wound in a spiral in the form of a sphere improves the breakdown threshold by a factor of about two over a cylindrical geometry. The frequency is measured with a Monsanto 105A counter to an accuracy of one part per million.

Figure 2 shows the double-resonance transition frequencies versus magnetic field for OH and OD. In the case of OH, resonances in the $F=2$ and $F=1$ hyperfine levels are observed. No deviations from linearity are detected to the highest frequencies to which we are able to follow the signal. The experimental g values are $g(F=1)=0.498\pm0.006$ and $g(F=2)=0.301\pm0.003$. These g values confirm, within experimental error, the theoretical g values for Hund's case $(b_{\beta J})$[13]:

$$g_F=\pm1/(N+\tfrac{1}{2})$$

$$\times\{[F(F+1)+J(J+1)-I(I+1)]/2F(F+1)\},\quad(1)$$

where $J=N\pm\tfrac{1}{2}$. Thus in the case of OH no information can be determined directly about the magnitude of the hyperfine splitting. In the case of OD, only one

resonance is seen which in the linear region corresponds to a g value of 0.383 ± 0.024, where the uncertainty is larger than for the OH g values because of the use of fewer double resonance measurements in the linear field region. This is assigned to the $F=\tfrac{5}{2}$ hyperfine component which for pure case $(b_{\beta J})$ has a theoretical value $g(F=\tfrac{5}{2})=0.400$. [In case $(b_{\beta J})g(F=\tfrac{3}{2})=22/45$, while $g(F=\tfrac{1}{2})=10/9$.] At higher fields, there is clearly a deviation from a linear Zeeman effect, as is apparent in Fig. 2(b). We expect OD to be a more favorable case than OH for observing intermediate field coupling because the smaller magnetic moment of D implies a smaller hyperfine splitting for OD. The double resonance measurements required one to two hour integration periods to obtain signal-to-noise ratios of about 4:1. Although some preliminary searches were made for other OD resonances, none were seen. In Sec. III.B we show that other resonances are expected to be much weaker in intensity.

In the course of these double resonance studies the relative intensities of the $F=1$ and $F=2$ resonances in OH are measured as a function of rf magnetic field at 7 MHz. The rf magnetic field strength is measured with an rf ammeter previously calibrated using a dc magnetic field. The results shown in Table I permit us to estimate the relative populations of the $F=2$ to the $F=1$ hyperfine levels to be 0.79 ± 0.18. This ratio is used in the determination of the OH radiative lifetime from the Hanle-effect data.

B. Zero-Field Level-Crossing Measurements

In the zero-field level-crossing studies the linewidth of the signal is used to measure the radiative lifetime of the A state. For the right-angle geometry shown in Fig. 1, the ideal theoretical line shape is an inverted Lorentzian for dc detection. In practice,
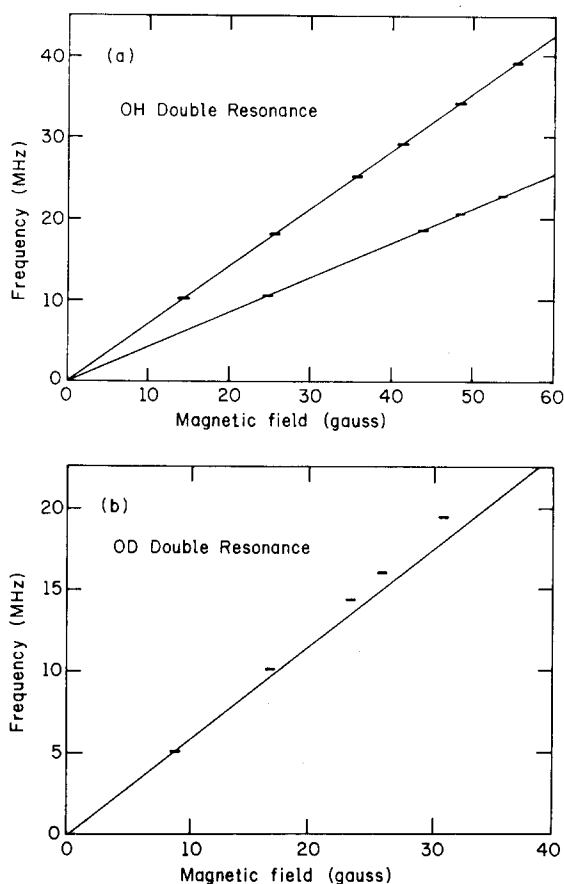
FIG. 2. Double-resonance transition frequencies for (a) OH and (b) OD as a function of magnetic field. The bars are the experimental data and the straight lines are the theoretical positions of the resonances using the g factors given by Eq. (1).

optical misalignment and the finite size of the source and detector add a small dispersion component in the limit of small modulation fields. At the finite modulation fields required to produce detectable signals, the line shape is broadened by the modulation. To extract the linewidth Γ, defined as the half-width

TABLE I. Relative intensities of the $F=2$ and $F=1$ double-resonance signals from the OH $A\,^2\Sigma^+$ $v=0$, $N=2$, $J=3/2$ level. The intensity ratio is determined at 7 MHz rf transition frequency at several different rf amplitudes. Column 3 is the calculated ratio of the two signals assuming equal populations in the $F=2$ and the $F=1$ hyperfine levels. Column 4 is the population ratio found by comparing Column 2 with Column 3.

rf Field amplitude (G)	$I(F=2)/$ $I(F=1)$ (measured)	$I(F=2)/$ $I(F=1)$ (calculated)	Population ratio $[F=2]/$ $[F=1]$
0.30	0.87	1.24	0.70
0.42	1.08	1.42	0.76
0.50	1.56	1.59	0.98
0.60	1.17	1.75	0.67
0.60	1.42	1.75	0.82

at half-maximum of the dc Lorentzian component, the level-crossing curves are fit by a nonlinear least-squares program to the expressions given in Eqs. (1) and (2) of an earlier paper on level-crossing studies in nitric oxide.[14] At zero pressure, Γ is related to the radiative lifetime τ and the magnetic moment $g\mu_0$ by
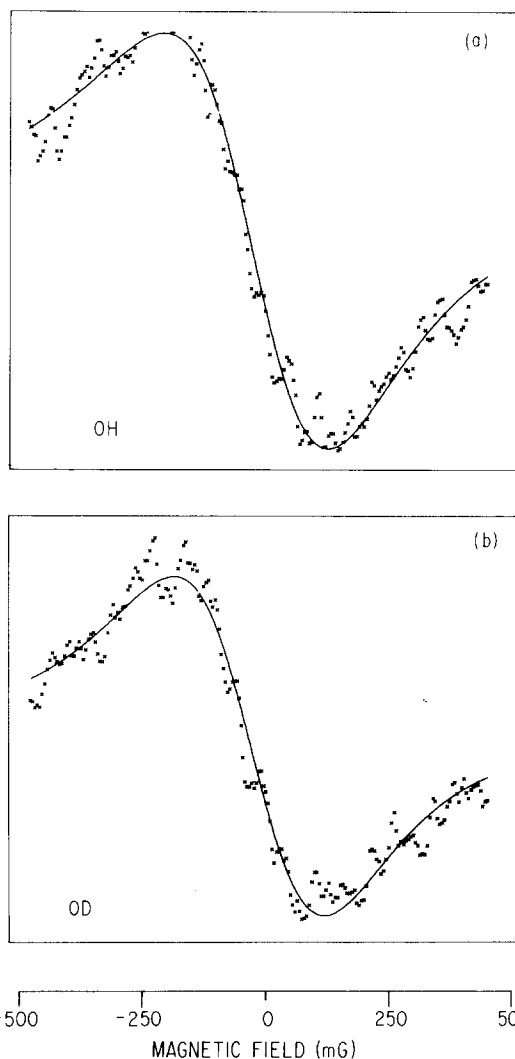
$$\Gamma = \hbar/2\mu_0 g\tau. \qquad (2)$$

FIG. 3. Hanle signal in (a) OH at 0.8 mtorr of H_2 and 0.65 mtorr of NO_2, and (b) in OD at 0.8 mtorr of D_2 and 0.90 mtorr of NO_2. The crosses are the data, and the smooth curve is the best nonlinear least-squares fit.

Figure 3 shows the results of these nonlinear fits for the lowest OH and OD pressures used in our determination of the zero-pressure value of Γ. At higher pressures, the signal-to-noise ratio is always better than that shown in Fig. 3, but collisions cause the value of Γ to be pressure-broadened. A simple model in which collisions merely randomize the phase of the emission oscillator requires us to replace τ in

Eq. (2) by the coherence time T, given by

$$T^{-1} = \tau^{-1} + n\kappa, \tag{3}$$

where n is the number density and κ is the rate constant for the destruction of alignment.

The linewidth Γ has been fit to Eq. (3) as a function of the pressure of both reactants, and the results are displayed in Figs. 4 and 5 for OH and OD, respectively. For OH and OD the data are well represented by a bilinear variation in reactant pressures, i.e.,

$$\Gamma(OH) = \Gamma^0(OH) + R_1[H] + R_2[NO_2] \tag{4}$$

and

$$\Gamma(OD) = \Gamma^0(OD) + R_3[D] + R_4[NO_2], \tag{5}$$

where

$\Gamma^0(OH) = 260$ mG; $\Gamma^0(OD) = 216$ mG;

$R_1 = 3.3$ mG/mtorr; $R_3 = 2.0$ mG/mtorr;

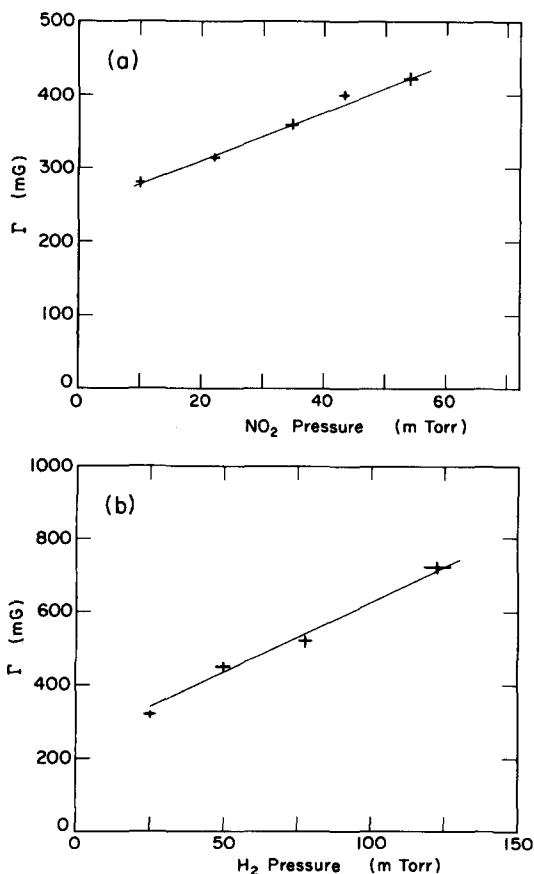$R_2 = 2.9$ mG/mtorr; $R_4 = 3.2$ mG/mtorr.

FIG. 4. OH Hanle-signal pressure-broadening data: (a) is for a fixed H_2 pressure at 7.2 mtorr; (b) is for a fixed NO_2 pressure at 5.6 mtorr. The data points are represented by crosses whose vertical dimension represents one standard deviation in the best fit to the theoretical line shape and whose horizontal dimension is the uncertainty in the pressure.

FIG. 5. OD Hanle-signal pressure-broadening data: (a) is for a fixed D_2 pressure at 17.0 mtorr; (b) is for a fixed NO_2 pressure at 2.7 mtorr. The data points are represented by crosses whose vertical dimension represents one standard deviation in the best fit to the theoretical line shape and whose horizontal dimension is the uncertainty in the pressure.
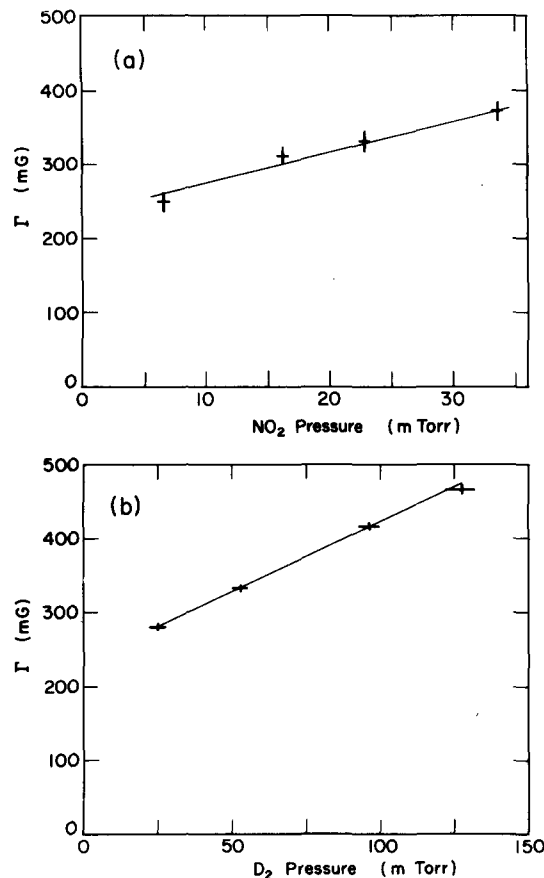
Low pressure data such as those shown in Fig. 3 give values for Γ^0 that are within 2% of the Γ^0 values found from the bilinear extrapolation. At the lowest pressure points, the OH concentration is less than a few tenths millitorr, and the amount of radiation trapping is calculated to be negligible. Even at the higher pressure, corresponding to the data shown in Figs. 4 and 5, the effects of radiation trapping will give little coherence narrowing because the transfer of coherence via the different rotational branches tends to cancel. Consequently, no correction is made to Γ^0 for the effects of coherence narrowing. The best averaged values are $\Gamma^0(OH) = 266 \pm 21$ mG and $\Gamma^0(OD) = 218 \pm 18$ mG.

Our determination of Γ^0 is subject to the following errors:

(1) Magnetic field calibration (0.1%).
(2) Uncertainty in the pressure measurements. These are twofold: (a) the gauge accuracy given by the manufacturer as 3%; and (b) the uncertainty

(2%) in the correction necessary to estimate the pressure in the reaction region caused by the fact that the gauge could not be placed in the reaction region.

(3) The statistical uncertainty in the pressure extrapolations. This is 3% per standard deviation in the case of OH and 5% per standard deviation in OD.

All uncertainties in the values of the pressures do not affect Γ^0 by more than 1%, but they do affect the pressure-broadening parameters R_1, R_2, R_3, and R_4. We assign an error of 9% (three standard deviations) to Γ^0(OH) and Γ^0(OD). It is difficult to assign an error estimate to the R parameters because this would require combining the systematic errors in the calibration with the statistical errors from the pressure extrapolation. Because the excited OH and OD molecules are not in the same quantum states, a comparison of the R values is difficult, although R_2 is approximately equal to R_4, as might be expected if the excited OH and OD molecules behave in a comparable manner. The interpretation of the R's is further complicated because collisional transfer to neighboring rotational levels is expected to make an important contribution to the apparent depolarization rate.

III. ANALYSIS OF DATA

To determine the hyperfine splitting from the double resonance data in OD, we must calculate the Zeeman energy levels of the Hamiltonian. The assignments of the observed rf resonances are obtained from double resonance theory. Following the analysis of the OD hyperfine structure, we extract radiative lifetimes from the OH and OD Hanle linewidths.

A. The Molecular Hamiltonian

In $^2\Sigma^+$ electronic states each rotational level N is split into two spin components $J=N\pm\frac{1}{2}$ separated by an amount $\gamma(N+\frac{1}{2})$, where γ is the rho-doubling constant. This fine structure splitting may be represented by the interaction term

$$H_{fs}=\gamma\mathbf{N}\cdot\mathbf{S}. \tag{6}$$

In the $A\,^2\Sigma^+$ states of OH and OD, the off-diagonal spin–orbit interaction with the $X\,^2\Pi$ state appears to account for most of the value of γ, as shown in Appendix A. There have been two spectroscopic determinations of the value of γ in the $v=0$ level of the A state of OD. Scarl and Dalby,[15] as part of their Stark studies of the ultraviolet bands of OD, report $\gamma=0.121\pm0.005$ cm^{-1}. More recently, Clyne, Coxon, and Woon Fat[16] have made a high resolution study of the (0, 0) band of the OD $A–X$ system from which their preliminary analysis yields $\gamma=0.1200\pm0.0023$ cm^{-1} where the uncertainty represents the spread in values of γ with fitting procedure. We accept the latter value as the more accurate determination of γ.

For a diatomic molecule with only one magnetically active nucleus, the hyperfine structure Hamiltonian was first derived by Frosch and Foley[17] with subsequent minor numerical corrections by Dousmanis.[18] For the $A\,^2\Sigma^+$ state of OH or OD the hyperfine splittings arise almost entirely from the interaction of the magnetic moment of the H or D nucleus with the unpaired electron spin density. In the case of OD there is also a small nuclear electric quadrupole interaction. To good approximation the hyperfine Hamiltonian is given by

$$H_{hfs}=b(\mathbf{I}\cdot\mathbf{S})+cI_zS_z+eQq[3I_z^2-I(I+1)]/4I(2I-1), \tag{7}$$

where

$$b=(\tfrac{16}{3}\pi)(\mu_0\mu_I/I)\Psi^2(0)-(\mu_0\mu_I/I)\langle(3\cos^2\theta-1)/r^3\rangle, \tag{8}$$

$$c=(3\mu_0\mu_I/I)\langle(3\cos^2\theta-1)/r^3\rangle, \tag{9}$$

and

$$q=\sum_i e_i\langle(3\cos^2\theta_i-1)/r_i^3\rangle. \tag{10}$$

Here θ is the angle between the molecular axis and the radius vector r from the magnetically active nucleus to the electron and the expectation values refer to an average taken over the unpaired electron charge distribution. Whenever there is an appreciable amount of $1s$ character to an unpaired electron about the magnetically active nucleus, the Fermi contact term, which is the first term in the expression for b, may be expected to dominate the magnitude of the splitting.

The matrix elements of H_{hfs} have been evaluated previously by Radford[19] in the case of $^2\Sigma$ states. For $N=1$, $I=1$, we have explicitly

$$\langle J=\tfrac{1}{2}\mid H_{fs}+H_{hfs}\mid J=\tfrac{1}{2}\rangle=(-b+c)(x^2-3)/6-3\gamma/4$$
$$-eQq[(x^2-3)(x^2-2)-1]/4,$$

$$\langle J=\tfrac{3}{2}\mid H_{fs}+H_{hfs}\mid J=\tfrac{3}{2}\rangle=\tfrac{1}{6}[(b+c/5)(x^2-6)]$$
$$+\tfrac{3}{4}\gamma-\tfrac{1}{4}\{eQq[\tfrac{1}{5}(x^2-5)(x^2-6)-1]\},$$

$$\langle J=\tfrac{1}{2}\mid H_{fs}+H_{hfs}\mid J=\tfrac{3}{2}\rangle=[b+\tfrac{1}{2}c+\tfrac{3}{10}eQq(x^2-\tfrac{7}{2})]$$
$$\times\tfrac{1}{6}[x(9-x^2)^{1/2}], \tag{11}$$

where $x=F+\tfrac{1}{2}$.

In the presence of a magnetic field a Zeeman term of the form

$$H_z=\mu_0(g_e\mathbf{S}+\mathbf{L})\cdot\mathbf{H}+\mu_N g_I\mathbf{I}\cdot\mathbf{H} \tag{12}$$

must be added to the Hamiltonian. In Eq. (12), the first term represents the interaction of the electronic spin and orbital angular momentum with the external magnetic field $\mathbf{H}$, and the second term is the analogous expression for the nuclear spin. Because μ_N is about 2000 times smaller than μ_0, the second term will be neglected. The contribution of the $\mathbf{L}\cdot\mathbf{H}$ term is zero for a pure Σ state, but a slight $^2\Pi$ admixture introduces small correction terms off-diagonal in Λ. An estimate

of the extent of $^2\Pi$ mixing may be obtained from the Λ-doubling parameters of the $X\,^2\Pi$ state[2,3] (as discussed in Appendix A), and we deduce that the corrections to the g_F values are $+0.2\%$ for $N=2$, $J=3/2$ of OH, and $+0.4\%$ for $N=1$, $J=3/2$ of OD. The matrix elements of the $\mathbf{S}\cdot\mathbf{H}$ term may be evaluated by standard means[20] from the expression

$$\langle SNJ'IF'M_F' \mid H_z \mid SNJIFM_F\rangle$$

$$= g_e\mu_0 H(-1)^{F'-M_{F'}+J'+I+F+S+N+J}$$

$$\times[(2F+1)(2F'+1)(2J+1)(2J'+1)(S)$$

$$(S+1)(2S+1)]^{1/2}$$

$$\times\begin{pmatrix} F' & 1 & F \\ -M_F' & 0 & M_F \end{pmatrix}\begin{Bmatrix} J' & F' & I \\ F & J & 1 \end{Bmatrix}\begin{Bmatrix} S & J' & N \\ J & S & 1 \end{Bmatrix}. \quad (13)$$

The double resonance experiments involve radio-frequency transitions between the ΔM_F levels satisfying the condition $\Delta M_F=\pm 1$. As long as the Zeeman splittings are much smaller than the hyperfine intervals, each transition with a hyperfine level has the same frequency at the same magnetic field and is characterized by the g value given by Eq. (1). However, at higher values of the magnetic field the transition frequencies within an F level are unequal, and it is necessary to diagonalize the full Hamiltonian in the above representation to find the dependence of each transition frequency on magnetic field.

B. Double Resonance and Level Crossing Intensities

To estimate the hyperfine splitting from the position of the OD double resonance signal in the nonlinear Zeeman region, it is necessary to assign the pair or pairs of $(F=5/2, M_F)$ levels responsible for the double resonance. Since the excitation is dominated by $\Delta F=\Delta J=0$ transitions, the $\mid M_F\mid=F$ sublevels are preferentially populated when using π-polarized light. Thus it is reasonable to expect that the $M_F=5/2\leftrightarrow M_F=3/2$ or the $M_F=-5/2\leftrightarrow M_F=-3/2$ transitions would be most intense. From computed energy levels based on trial values of $b+c/5$ (we neglect eQq in what follows) the $M_F=-5/2\leftrightarrow M_F=-3/2$ and the $M_F=-3/2\leftrightarrow M_F=-1/2$ transitions deviate to higher frequency as a function of magnetic field showing the same trend as our data [see Fig. 2(b)]. This suggests that the most likely assignment of the double resonance signal is to the $M_F=-5/2\leftrightarrow M_F=-3/2$ transition.

To confirm this assignment as well as to explain why other resonances were not detected, we calculated the intensities of the double resonance signals in intermediate field by generalizing the existing theory of double resonance. Intensity expressions are also developed in this section for the determination of the relative contribution of each hyperfine level to the zero-field level crossing.

Optical radio-frequency double resonance intensities

in the region of the linear Zeeman effect have been discussed by many authors.[12,21–24] The fluorescence intensity may be expressed as

$$I=\mathrm{Tr}[\varrho\mathfrak{M}] \quad (14)$$

where ϱ is the steady-state density matrix for the excited state and $\mathfrak{M}$ is the so-called monitoring operator. The elements of ϱ for a given hyperfine level F are obtained from Eq. (22) of Carver and Partridge's review article[22]:

$$\rho_{MM'}=W\sum_{M_0,M_0',N,N'}\rho_{M_0M_0'}{}^0$$

$$\times\exp[-i(M-M'+M_0'-M_0)\omega t/2]$$

$$\times\frac{d_{MN}^F(\theta)d_{NM_0}^F(-\theta)d_{M_0'N'}^F(\theta)d_{N'M'}^F(-\theta)}{\Gamma+i[(M_0-M_0')\omega_0+(N-N')p]}. \quad (15)$$

Here $\rho_{M_0M_0'}{}^0$ is the density matrix immediately after excitation,

$$\rho_{M_0M_0'}{}^0=\sum_{F''J''M''}\langle FJM_0\mid \boldsymbol{\mu}\cdot\boldsymbol{\varepsilon}_i\mid F''J''M''\rangle$$

$$\times\langle F''J''M''\mid \boldsymbol{\mu}\cdot\boldsymbol{\varepsilon}_i\mid FJM_0'\rangle, \quad (16)$$

where $\boldsymbol{\mu}$ is the transition dipole moment operator and $\boldsymbol{\varepsilon}_i$ is the polarization vector of the incident light. The summation in Eq. (16) runs over all ground state levels $F''J''M''$ that are connected by optical transitions to the excited state within the lamp profile. The other quantities appearing in Eq. (15) are defined as in Carver and Partridge. The matrix elements of the monitoring operator are given by

$$\mathfrak{M}_{M'M}=\sum_{F'''J'''M'''}\langle FJM'\mid \boldsymbol{\mu}\cdot\boldsymbol{\varepsilon}_f\mid F'''J'''M'''\rangle$$

$$\times\langle F'''J'''M'''\mid \boldsymbol{\mu}\cdot\boldsymbol{\varepsilon}_f\mid FJM\rangle, \quad (17)$$

where $F'''J'''M'''$ are the terminal ground state levels and $\boldsymbol{\varepsilon}_f$ is the polarization vector of the fluorescent light.

The state labels F and J appearing in Eqs. (16) and (17) are almost good quantum numbers; they are used here to denote the eigenfunctions of the Hamiltonian. The dipole matrix elements appearing in $\mathfrak{M}$ and ϱ may be computed in the pure $FMJ\Lambda\Sigma$ representation,[25] namely

$$\sum_{p=-1}^{1}\langle FMJ\Lambda\Sigma\mid \mu_p\varepsilon_p\mid F'M'J'\Lambda'\Sigma'\rangle$$

$$=\sum_{p=-1}^{1}(-1)^{F-M}\begin{pmatrix} F & 1 & F' \\ -M & p & M' \end{pmatrix}(-1)^{I+J'+F+1}$$

$$\times[(2F+1)(2F'+1)]^{1/2}\begin{Bmatrix} I & J & F \\ 1 & F' & J' \end{Bmatrix}$$

$$\times(-1)^{J-\Omega}[(2J+1)(2J'+1)]^{1/2}$$

$$\times\begin{pmatrix} J & 1 & J' \\ -\Lambda-\Sigma & \Lambda-\Lambda' & \Lambda'+\Sigma' \end{pmatrix}\langle\Lambda\mid\mid\mu\mid\mid\Lambda'\rangle. \quad (18)$$

By expressing the $|FJM\rangle$ wavefunctions as linear combinations of the pure $|FMJ\Lambda\Sigma\rangle$ basis, the dipole matrix elements appearing in Eqs. (16) and (17) are evaluated with the help of Eq. (18).

Let us first specialize these results to our double resonance experiment. Since we use π-polarized light in excitation and in detection, we only need to consider the $p=0$ component, μ_z, in Eq. (18). Hence ϱ^0 is a diagonal matrix. Furthermore, since we observe only the unmodulated component of the double resonance signal, $M=M''$ and ϱ is also a diagonal matrix, i.e.,

$$\rho_{MM} = W \sum_{M_0, N, N'} \rho_{M_0 M_0}{}^0$$

$$\times \frac{d_{MN}{}^F(\theta) d_{NM_0}{}^F(-\theta) d_{M_0 N'}{}^F(\theta) d_{N'M}{}^F(-\theta)}{\Gamma + i(N-N')p}. \quad (19)$$

In the intermediate field region the nonlinearities in the Zeeman effect cause the $\Delta F=0$, $\Delta M_F=\pm 1$ transitions to be resolved. Equations (14)–(17) may be applied formally to each resonance as though it were a separate two-level system $(S=\frac{1}{2})$. The effective g value or magnetic dipole transition moment is computed by calculating the expectation value of the rf interaction $-\boldsymbol{\mu}\cdot\mathbf{H}_{rf}$, using the eigenfunctions appropriate to intermediate field. The change in the fluorescent intensity induced by the rf field for a system with two levels 1 and 2 is given by

$$\Delta I_{12} = \mathrm{Tr}[\rho\mathfrak{M}] - \mathrm{Tr}[\rho^0\mathfrak{M}]$$

$$= (\rho_{11} - \rho_{11}{}^0)\mathfrak{M}_{11} + (\rho_{22} - \rho_{22}{}^0)\mathfrak{M}_{22}. \quad (20)$$

The effect of the rf field is to redistribute the populations in the two levels, so that

$$\rho_{11} = \rho_{11}{}^0\{1 - [2\omega_1{}^2/(\Gamma^2 + 4\omega_1{}^2 + \delta^2)]\}$$

$$+ \rho_{22}{}^0[2\omega_1{}^2/(\Gamma^2 + 4\omega_1{}^2 + \delta^2)], \quad (21)$$

with a similar expression for ρ_{22}.

In Eq. (21) $\omega_1 = \frac{1}{2}\langle 1 | \boldsymbol{\mu}\cdot\mathbf{H}_{rf} | 2\rangle$, where $\mathbf{H}_{rf}$ is the component of the rf field which rotates at frequency $\omega/2\pi$ and $\delta = \omega - \omega_0$, where $\omega_0/2\pi$ is the resonance frequency for the $1\leftrightarrow 2$ transition. When these expressions for ρ_{11} and ρ_{22} are substituted into Eq. (20) we find that

$$\Delta I_{12} = -2[\rho_{11}{}^0 - \rho_{22}{}^0][\mathfrak{M}_{11} - \mathfrak{M}_{22}][\omega_1{}^2/(\Gamma^2 + 4\omega_1{}^2 + \delta^2)].$$

$$(22)$$

A similar expression has been derived previously for rf electric dipole transitions.[26,27]

We have computed the population difference $[\rho_{11}{}^0 - \rho_{22}{}^0]$, the detection selectivity $[\mathfrak{M}_{11} - \mathfrak{M}_{22}]$, and the rf transition factor $2\omega_1{}^2/(\Gamma^2 + 4\omega_1{}^2 + \delta^2)$ for all pairs of F, M_F levels within the accessible field-frequency region, using trial values for the hyperfine splittings which in first order are proportional to $b+c/5$.

Although the rf transition elements, ω_1, are nearly the same value, there are marked variations in the population differences and detection selectivities for pairs of F, M_F levels. Figure 6 gives the theoretical intensities computed with the final fitted value for $b+c/5$ for fixed-frequency scans at 10 and 20 MHz for the $F=\frac{5}{2}$ manifold. From this figure it is seen that the intensity of the $M_F = -\frac{5}{2}\leftrightarrow M_F = -\frac{3}{2}$ transition is a factor of 2 or more times stronger than any other $(F=\frac{5}{2})$ rf transition and a factor of 10 times stronger than the $M_F = -\frac{3}{2}\leftrightarrow M_F = -\frac{1}{2}$ rf transition, thus confirming the assignment conjectured above and explaining why additional resonances were not observed. Calculations for the $F=\frac{3}{2}$ and $F=\frac{1}{2}$ manifolds show that resonances in these manifolds are expected to be at least two times weaker, and hence not readily detectable with our experimental signal-to-noise ratio. No concerted effort was made to find other resonances.

We now turn our attention to the development of intensity expressions we will use later to analyze the level crossing data. In the absence of an rf field, $\omega_1 = \omega = 0$, and Eqs. (14) and (15) yield the familiar Breit equation for the intensity of the fluorescence:

$$I = \sum_{F, J, M_0, M_0'} \frac{\langle FJM_0 | \rho^0 | FJM_0'\rangle\langle FJM_0' | \mathfrak{M} | FJM_0\rangle}{\Gamma + i(M_0 - M_0')\omega_0{}^F}$$

$$(23)$$

In using Eq. (23) to determine the relative contribution of different hyperfine levels to the Hanle signal, a lamp profile factor must in general be included in the calculation of ρ^0. The profile factor is important in the case of the Zn line excitation of $v=2$, $J=\frac{3}{2}$ level of OH, as will be discussed in Sec. D. We have used the double resonance intensities for the $F=1$ and $F=2$ levels at 7 MHz, as given in Table I, to determine their relative contributions to the Hanle effect. The relationship between the resonance intensities in the linear Zeeman region and the Hanle effect signals is most conveniently expressed by a multipole expansion for each hyperfine level F similar to that presented by Happer and Saloman.[23] Because of the elegant simplification this formalism provides, a brief review follows.

The density matrix and monitoring operators of Eqs. (16) and (17) may be expanded in multipoles of order L:

$$\rho^0 = \sum_{F, L} \rho_F(L) \sum_M (-1)^M E_i(L, -M) T_F(L, M) \quad (24)$$

and

$$\mathfrak{M} = \sum_{F, L} \mathfrak{M}_F(L) \sum_M (-1)^M E_f(L, -M) T_F(L, M). \quad (25)$$

For linearly polarized electric dipole excitation and fluorescence, only the $L=0$ and $L=2$ terms occur in Eqs. (24) and (25). The $L=0$ (monopole) terms express the average population and detection of the
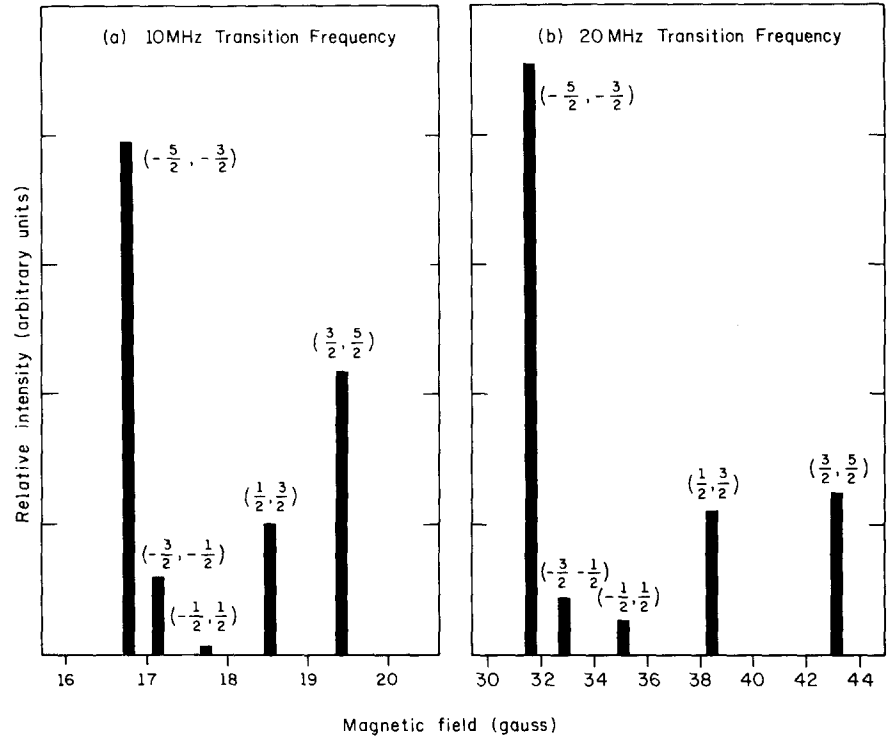
FIG. 6. Relative intensities for double-resonance transitions (M_1, M_2) in the $F = \frac{5}{2}$ hyperfine component at (a) 10 MHz transition frequency and (b) 20 MHz transition frequency, calculated using $b + c/5 = 121$ MHz.

excited state magnetic sublevels within a hyperfine level F. The $L = 2$ (quadrupole) terms express the alignment of the excited state, namely the population and detection differences between the $|M|$ and $|M-1|$ magnetic sublevels. The polarization tensors in absorption, E_i, and in fluorescence, E_f, are determined by the respective polarization vectors $\mathcal{E}_i$ and $\mathcal{E}_f$ through the relation

$$E(L, M) = \sum_\mu \mathcal{E}_\mu \mathcal{E}_{\mu-M}^* (-1)^{1-\mu} (2L+1)^{1/2}$$

$$\times \begin{pmatrix} 1 & 1 & L \\ \mu & M-\mu & -M \end{pmatrix}. \quad (26)$$

The irreducible tensor $T_F(L, M)$ expresses the transformation from the $(2F+1)^2$ elements of the $|FM_F\rangle \times \langle FM_F'|$ basis to the elements of the (L, M) basis:

$$T_F(L, M) = \sum_{M_F} |FM_F\rangle \langle FM_F - M|$$

$$\times (-1)^{F-M_F} (2L+1)^{1/2} \begin{pmatrix} F & F & L \\ M_F & M-M_F & -M \end{pmatrix}. \quad (27)$$

In a double resonance experiment that employs π-polarized light in excitation and detection, such as we have carried out, the only nonvanishing elements of the polarization tensors are $E_i(0, 0) = E_f(0, 0) = (1/3)^{1/2}$ and $E_i(2, 0) = E_f(2, 0) = -(2/3)^{1/2}$. Because of the complexity of the transition elements and the multitude of radiative branches, it is convenient for

molecular systems to calculate $\rho_F(L)$ by projection from ρ^0, where ρ^0 has been obtained using Eqs. (16) and (18). We find that

$$\rho_F(L) E_i(L, M) = \text{Tr}[\rho^0 T_F(L, M)], \quad (28)$$

where we make use of property of $T_F(L, M)$ that

$$\text{Tr}[(-1)^{M'} T_F(L, M) T_F(L', -M')] = \delta_{LL'} \delta_{MM'}. \quad (29)$$

An analogous projection equation holds for $\mathfrak{M}_F(L)$.

In the above notation the Breit equation has the form

$$I = \sum_{F,L} \rho_F(L) \mathfrak{M}_F(L) \sum_M (-1)^M$$

$$\times \frac{E_i(L, M) E_f(L, -M)}{1 + iM\omega_0{}^F/\Gamma}. \quad (30)$$

For a right angle geometry and with unpolarized light in excitation and in detection, the Hanle signal is

$$\Delta I = -\frac{1}{2} \sum_F \frac{\rho_F(2) \mathfrak{M}_F(2)}{1 + (2\omega_0{}^F/\Gamma)^2}. \quad (31)$$

In these expressions we assume equal decay rates, Γ, for all multipole orders.

In the same notation, it may be shown (See Appendix B) that the unmodulated double resonance signal for a given hyperfine level, F, with π-polarized excitation and detection is

$$I_F = \sum_L \rho_F(L) \mathfrak{M}_F(L) E_i(L, O) E_f(L, O)$$

$$\times \sum_{M'} [d_{OM'}{}^L(\theta) d_{M'O}{}^L(-\theta)/(\Gamma - iM'p)]. \quad (32)$$

Only the $L=2$ multipole terms are affected by the rf field and the signal at resonance (See Appendix B) is

$$\Delta I_F = -2\frac{\rho_F(2)\mathfrak{M}_F(2)\omega_1^2}{1+(2\omega_1/\Gamma)^2}, \qquad (33)$$

where $\omega_1 = \mu_0 g_F H_{rf}$. Because $\rho_F(2)\mathfrak{M}_F(2)$ is common to the terms in the Hanle signal and the double resonance signal for the F hyperfine level, Eqs. (30) and (32) serve as the basis for an experimental determination of the lamp profile factor in ρ^0.

C. Analysis of the Double Resonance Data

Once the OD double resonance signal has been assigned, the transition frequency may be calculated from the Hamiltonian using Eqs. (11) and (13). For the $J=\frac{3}{2}$, $F=\frac{5}{2}$, $M_F=-\frac{5}{2}$ component, the energy (neglecting eQq) is given by

$$E(\tfrac{3}{2},\tfrac{5}{2},-\tfrac{5}{2})=3\gamma/4+\tfrac{1}{2}(b+c/5)-\mu_0 H. \qquad (34)$$

Note that $E(\tfrac{3}{2},\tfrac{5}{2},-\tfrac{5}{2})$ varies linearly with magnetic field. For the $M_F=-\frac{3}{2}$ component the energy levels are the roots of the secular determinant

$$\begin{vmatrix}
|\tfrac{3}{2},\tfrac{5}{2},-\tfrac{3}{2}\rangle & |\tfrac{3}{2},\tfrac{3}{2},-\tfrac{3}{2}\rangle & |\tfrac{1}{2},\tfrac{3}{2},-\tfrac{3}{2}\rangle \\
\tfrac{3}{4}\gamma+\tfrac{1}{2}(b+c/5)-\tfrac{3}{5}\mu_0 H-E & [(24)^{1/2}/15]\mu_0 H & [-2(30)^{1/2}/15]\mu_0 H \\
[(24)^{1/2}/15]\mu_0 H & \tfrac{3}{4}\gamma-\tfrac{1}{3}(b+c/5)-\tfrac{11}{15}\mu_0 H-E & [(5)^{1/2}/3](b+c/2)-[4(5)^{1/2}/15]\mu_0 H \\
[-2(30)^{1/2}/15]\mu_0 H & [(5)^{1/2}/3](b+c/2)-4(5)^{1/2}/15]\mu_0 H & -\tfrac{3}{4}\gamma-\tfrac{1}{6}(b+c)+\tfrac{1}{3}u_0 H-E
\end{vmatrix}=0,$$

$$(35)$$

and the dependence on magnetic field is nonlinear.

The data shown in Fig. 2(b) are fit to the difference between Eq. (34) and the appropriate eigenvalue of Eq. (35) to provide and estimate for the quantity $b+c/5$. In carrying out this computation we set $c=25$ MHz, the value determined by a restricted Hartree–Fock calculation.[28] Because the value of c is small compared to b, the quantity $b+c/5$ found in this manner is essentially independent of the choice of c. The least squares fit yields a value

$$b+c/5=121\pm14 \text{ MHz} \qquad (36)$$

from which we estimate $b=116\pm14$ MHz. The theoretical value of c is believed to be accurate to better than ±5 MHz, so that its uncertainty has not been included in the estimate of b.

D. Determination of Lifetimes from Hanle Effect Data

To extract the radiative lifetime, we must take into account the relative contribution of each excited state hyperfine level to the observed level crossing signal. In the case of OD, we excite the three hyperfine components $F=\frac{5}{2}$, $\frac{3}{2}$, and $\frac{1}{2}$ of the $N=1$, $J=\frac{3}{2}$ rotational level. However, the $F=\frac{1}{2}$ component cannot contribute to the Hanle signal for excitation by unpolarized light.[11] The case $(b_{\beta J})$ g values of the components are $g(F=\frac{5}{2})=\frac{2}{5}$ and $g(F=\frac{3}{2})=\frac{22}{45}$. From Eq. (23) or (31), with the assumption of a flat spectral profile of the lamp, we find that the relative strengths of the Hanle signal for these two components are

$$I(F=\tfrac{3}{2})/I(F=\tfrac{5}{2})=0.045. \qquad (37)$$

The uncertainty caused by the variation in the lamp profile for the OD lifetime studies is not significant because (1) the Hanle signal arising from the $F=\frac{3}{2}$ component is more than 20 times larger than the $F=\frac{5}{2}$ component, (2) the hyperfine transitions span only a small fraction of the Doppler width of the lamp, and (3) the g_F values of the two components are similar.

It is sufficiently accurate in this case to fit the Hanle signal to a single Lorentzian with an adjustable width where the width is proportional to the product of an effective g value and the radiative lifetime τ as was described in Sec. II.B. The value of g_{eff} is obtained by weighting the respective g factors by the relative contributions from the two hyperfine components. Using a value of $g_{eff}=0.404$, we obtain from $\Gamma^0(OD)$ the radiative lifetime

$$\tau(OD)=0.65\pm0.06 \ \mu sec$$

for the $v=0$, $N=1$, $J=\frac{3}{2}$ level of the $A\,^2\Sigma^+$ state of OD.

On the other hand, the interpretation of the Hanle effect observed in the $N=2$, $J=\frac{3}{2}$ level of the $A\,^2\Sigma^+$ state of OH requires a more involved treatment. The $F=1$ and $F=2$ hyperfine levels have the g values $g(F=1)=0.5$ and $g(F=2)=0.3$. Furthermore, the computed relative intensities for a flat spectral profile

TABLE II. Experimentally determined values of f_{00} and $\tau_{v'=0}$ for the OH $A\ ^2\Sigma^+$-$X\ ^2\Pi$ band system.

Investigator[a]	Method of OH production	Method of measurement	Resolution of rotational lines	$f_{00} \times 10^{-4}$	τ (μsec) [d]
Oldenberg and Rieke (1938)	Thermal dissociation	Integrated absorption coefficient	yes	9.5 ± 1.0[b]	0.80 ± 0.11
Dwyer and Oldenberg (1944)					
Dyne (1958)	Thermal dissociation	Integrated absorption coefficient	yes	5.4 ± 1.0[b]	1.41 ± 0.26
		Curve of growth	yes	4.9 ± 1.0[b]	1.55 ± 0.31
Carrington (1959)	Flame	Curve of growth	yes	11.1 ± 5.0[b]	0.686 ± 0.31
Lapp (1961)	Reflected shock	Band emission	no	10 ± 6[b]	0.76 ± 0.45
Del Greco and Kaufman (1962)	$H + NO_2$ flow system	Line absorption	yes	5.6 ± 1.2	1.36 ± 0.29
Golden, Del Greco, and Kaufman (1963)	$H + NO_2$ flow system	Line absorption	yes	7.1 ± 1.1	1.07 ± 0.16
Watson (1964)	Reflected shock	Band emission	no	39 ± 9	0.195 ± 0.045
Bennett and Dalby (1964)	Electron impact dissociation of H_2O, CH_3OH	Phase shift	no	8.0 ± 0.8	1.01 ± 0.05
Bird and Schott (1965)	Reflected shock	Line absorption	yes	12.8[c]	5.95
Anketell and Perry-Thorne (1967)	Thermal dissociation	Hook method	yes	14.8 ± 1.3	0.514 ± 0.045
Smith (1970)	Electron impact dissociation of H_2O	Phase shift	no	8.9 ± 1.4	0.85 ± 0.13
deZafra, Marshall, and Metcalf (1971)	$H + NO_2$ flow system	Hanle effect molecular lamp excitation	yes	11.5 ± 0.38	0.660 ± 0.022
This work	$H + NO_2$ flow system	Hanle effect line excitation	yes	13.1 ± 1.1	0.58 ± 0.05

[a] References to Table II in chronological order: (1) O. Oldenberg and F. F. Rieke, J. Chem. Phys. 6, 439 (1938); (2) R. J. Dwyer and O. Oldenberg, J. Chem. Phys. 12, 351 (1944); (3) P. J. Dyne, J. Chem. Phys. 28, 999 (1958); (4) T. Carrington, J. Chem. Phys. 31, 1243 (1959); (5) M. Lapp, J. Quant. Spectry. Radiative Transfer 1, 30 (1961); (6) F. P. Del Greco and F. Kaufman, Discussions Faraday Soc. 33, 128 (1962); (7) D. M. Golden, F. P. Del Greco, and F. Kaufman, J. Chem. Phys. 39, 3034 (1963); (8) R. Watson, J. Quant. Spectry. Radiative Transfer 4, 1 (1964); R. Watson and W. R. Ferguson, *ibid.* 5, 595 (1965); (9) R. G. Bennett and F. W. Dalby, J. Chem. Phys. 40, 1414 (1964); (10) P. F. Bird and G. L. Schott, J. Quant. Spectry. Radiative Transfer 5, 783 (1965); (11) J. Anketell and A. Perry-Thorne, Proc. Roy. Soc. (London) A301, 343 (1967); (12) W. H. Smith, J. Chem. Phys. 53, 792 (1970); (13) R. L. deZafra, A. Marshall, and H. Metcalf, Phys. Rev. A 3, 1557 (1971).

[b] As recomputed by Anketell and Perry-Thorne with corrections for the dissociation energy of OH and vibration–rotation interaction.

[c] Bird and Schott assign no error to their measurement.

[d] The value of τ is an average over the rotational levels observed (see text).

are more nearly comparable:

$$I(F=1)/I(F=2) = 0.40. \qquad (38)$$

The separation between the two hyperfine components based on the above value of the OD hyperfine splitting places the $F=2$ component 300 ± 30 MHz below the $F=1$ component. Consequently, the spectral range of the hyperfine transitions is significant with respect to the Doppler linewidths of the lamp and of the molecule.

An estimate of the lamp profile factor may be obtained from the relative intensities of the $F=1$ and $F=2$ double resonance signals, as discussed in Sec. II.C. Table I shows, for several values of the rf magnetic field, the observed double resonance intensity ratios at 7 MHz, the ratios computed from Eq. (33) using

the assumption of a flat profile, and the derived lamp profile factor. We conclude the $F=2$ is less strongly pumped than $F=1$ by a factor of 0.79 ± 0.17. It is interesting to note that this agrees qualitatively with the Zeeman scan of the Zn line published by Hollander and Broida.[29] Their Fig. 1 indicates that the center of the Zn line is ~ 0.05 cm^{-1} to the short wavelength side of $N=2$, $J=\frac{3}{2}$, and therefore, in view of the small ground state hyperfine splitting, pumps $F=1$ more than $F=2$.

With the experimentally determined lamp profile factor the value for g_{eff} is calculated to be 0.367 from which we obtain from $\Gamma^0(OH)$ the value

$$\tau(OH) = 0.58 \pm 0.05 \ \mu\text{sec} \qquad (39)$$

for the $v=0$, $N=2$, $J=\frac{3}{2}$ level of the $A~^2\Sigma^+$ state of OH.

Ideally, the experimental Hanle signals should be fit to a sum of two Lorentzians where the amplitudes of the $F=1$ and the $F=2$ Lorentzians are in the ratio 1.98 to 1 and their widths in the ratio 0.3 to 0.5. We have refit the data by this procedure but found no systematic change in the value of τ to within 1%.

IV. DISCUSSION

A. Lifetime Measurements

A variety of methods have been used to measure lifetimes and oscillator strengths in the $A~^2\Sigma^+$ state of OH and the results are summarized in Table II. To compare the findings of different investigators it is necessary to relate the oscillator strength f_{00} and the lifetime τ. Although the (0, 0) band of the $A-X$ system in OH and in OD have Franck–Condon factors[30] of 0.908 and 0.881, respectively, there is convincing evidence from intensity measurements[1,31] and from the computed dependence of the electronic transition moment with internuclear distance[32] that at least 99% of the fluorescence intensity from $v'=0$ is emitted in the (0, 0) band, for both OH and OD. In such a case, f_{00} and τ for a Σ–Π transition are related by the simple expression

$$f_{00} = 0.7995/\tau\nu_{00}^2, \qquad (40)$$

where ν_{00} is the frequency in cm^{-1} of the (0, 0) band and τ is the lifetime in seconds. Table II has been constructed using this relation. In particular, with our previously determined values of τ(OH) and τ(OD) we find that

$$f_{00}(\text{OH}) = 1.31 \pm 0.11 \times 10^{-3} \qquad (41)$$

and

$$f_{00}(\text{OD}) = 1.17 \pm 0.10 \times 10^{-3}. \qquad (42)$$

On examining Table II, a wide variation of reported lifetimes (oscillator strengths) is apparent, even among measurements taken within the past 10 years. However, there is mounting evidence that the radiative lifetime varies significantly with J. Accordingly, comparison between the results of different workers may not be meaningful unless it is known which rotational levels are observed. The precise magnitude of this variation is not well determined. Anketell and Pery-Thorne[33] report a $7\pm3\%$ increase of oscillator strength from $N=10$ to $N=1$, based on Hook-method measurements of resolved absorption lines. Moreover, results communicated to us by Smith,[34] who measured the radiative lifetime of resolved rotational lines using pulsed electron excitation and the phase-shift method, show that τ decreases from 0.85 μsec for the entire unresolved (0, 0) band to 0.67 ± 0.09 μsec for the $N=4$ level. A similar marked dependence of τ with N is found by Anderson,[35] who used a pulsed rf discharge

and a delayed-coincidence detection method. At our suggestion, Metcalf and deZafra have reanalyzed their OH Hanle-effect data.[5] They find an apparent increase of perhaps 10% in τ as N varies from $N=2$ to $N=5$. In fact for $N=2$, their value of τ(OH) = 0.62 ± 0.08 μsec (three standard deviations) is in good agreement with our value of τ(OH) = 0.58 ± 0.05 μsec.

Because the electronic transition moment for this molecular band system has a strong dependence on internuclear distance, changes in the upper and lower state vibrational wavefunctions caused by vibration–rotation interaction (centrifugal distortion) result in appreciable variation of f_{00} and τ with N. To estimate the magnitude of this effect, Anketell and Lerner[36] have fit relative band intensity data to a transition moment variation of the form[37] $\exp(-\alpha r)$ where $\alpha = 5.97\pm0.15$ Å^{-1}. They find that this gives a 14% increase in the value of f_{00} when N decreases from $N=10$ to $N=1$. A counterbalancing contribution of one-half this magnitude from rotational-electronic mixing is then postulated[36] to account for the discrepancy between this increase and the $7\pm3\%$ increase observed by Anketell and Pery-Thorne.[33] We consider in Appendix A the effect of mixing of the $X~^2\Pi$ state with the $A~^2\Sigma^+$ state, which would appear to be the most likely source of this effect. However, we find that such rotational–electronic mixing introduces a negligible variation of f_{00} or τ with N. In the light of the observed[34] 26% increase of lifetime from low N to band-averaged values (for which a mean value of $N=15$ is suggested), and in the absence of a mechanism for the postulated rotational–electronic mixing, it appears that the variation of the oscillator strength and lifetime with $N(N+1)$ may be larger than that deduced from the hook method studies,[33] which contain considerable scatter. The observed lifetime variation is more consistent with the value of $[N(N+1)/110]\times 14\%$ derived from band intensity data.

In comparing our OH and OD lifetimes, we have inserted exponential variation of the electronic transition moments given above into the vibrational overlap calculations. We find that the oscillator strength for OH is computed to be only 2.3% larger than for OD, whereas we find f_{00}(OH) is about 10% larger than f_{00}(OD). We believe that the 10% difference between f_{00}(OH) and f_{00}(OD) mostly reflects experimental uncertainties in this method, as suggested by the assigned error limits.

In conclusion, the radiative lifetime of the $v'=0$ level of the $A~^2\Sigma^+$ state of OH and OD seems to be well established, at least for low N, by level crossing and double resonance studies using both atomic and molecular excitation sources. This value of $\tau(f_{00})$ can then serve as a check on *ab initio* calculations. So far, there has been only one calculation of f_{00}. Henneker and Popkie[32] used RHF–SCF wavefunctions for both the A and X states and they found f_{00}(OH) = 2.0×10^{-3}.

This calculated oscillator strength is about 50% larger than our f_{00} value. This suggests that configuration interaction calculations will be needed to account for the oscillator strength of this molecular band system.

B. Hyperfine Structure Measurements

The use of optical radio-frequency double resonance spectroscopy to obtain molecular parameters by following the double resonance signal as a function of magnetic field is a recent development.[4,5] In this work, we report the extension of double resonance measurements into the nonlinear Zeeman region in which the beginning of $\mathbf{I} \cdot \mathbf{S}$ uncoupling is observed. An analysis of the deviation of the Zeeman levels from linearity yields $b+c/5=121\pm14$ MHz for the $v=0$ level of the OD $A\,^2\Sigma^+$ state. To our knowledge, this represents the first hyperfine structure determination using this technique. While we were completing this study, we learned that this same method has been applied to measure the fine structure separations in the $v=0$, $N=1$, $I=0$ level of the $(1s\,3p)\,^3\Pi_u$ state of H_2 (the upper state of the Fulcher band system) in which the beginning of $\mathbf{N} \cdot \mathbf{S}$ uncoupling is observed.[38]

By following only one resonance into the nonlinear Zeeman region, we have been able to determine only one "lumped" parameter $b+c/5$. In principle, similar observation of other resonances would permit a determination of the separate hyperfine parameters. We chose instead to follow an alternative procedure in which knowledge of the hyperfine splitting is used to predict the locations and intensities of high-field level crossings. A search for these crossings was made and the results are presented in the following paper.[7] We defer until then a more detailed discussion of the origin of the hyperfine splitting.

However, our value of $b+c/5$ for the $v=0$ level of the OD $A\,^2\Sigma^+$ state permits us to estimate the hyperfine splitting in the corresponding state of OH by scaling our number by the ratio of the nuclear moments. In this manner we find for example hyperfine splittings in the $v=0$, $N=1$ OH $A\,^2\Sigma^+$ state of 509 MHz for $J=\frac{3}{2}$ and 227 MHz for $J=\frac{1}{2}$.

Litvak et al.[39] have proposed an ultraviolet pumping model to account for the OH maser action observed in the interstellar medium. In this model it is necessary for the hyperfine splittings to be much larger than the uv Doppler widths for the A state, estimated to be between 1 and 10 GHz.[40] Our estimate of the A state hyperfine splittings of OH requires a reassessment of the applicability of this model.

APPENDIX A: $(A\,^2\Sigma^+,\ X\,^2\Pi)$ MIXING

The $X\,^2\Pi$ ground state interacts with the $A\,^2\Sigma^+$ state through off-diagonal matrix elements of the spin–orbit and the nuclear rotation operator (Coriolis coupling). Julienne, Krauss, and Donn[41] have suggested that the interaction of $v=1$ and higher levels of the A state with the unbound levels of the X state provide a mechanism for the formation of OH in the interstellar medium through inverse predissociation. Our concern with this electronic mixing is twofold: (1) the (A, X) interaction introduces a correction to the excited-state Zeeman energies that might affect the interpretation of the double resonance data, and (2) the (A, X) interaction also alters the A–X electronic transition moment, which might contribute to its J dependence. The latter may constitute the rotational–electronic mixing conjectured by Anketell and Learner[36] to explain the discrepancies from simple centrifugal distortion corrections. In distinction to inverse predissociation, the above two effects result almost exclusively from the interaction of the A state with the bound vibrational levels of the X state, especially $v''=0$.

Within the $v=0$ turning points of the A state the $X\,^2\Pi$ state is the only other known bond state. Furthermore, the Λ doubling of the X state and the rho-type doubling of the A state are consistent to 5% with the same (A, X) interaction parameters. Therefore, we assume that to good approximation the electronic mixing is simply a two-state problem.

The matrix elements connecting a $^2\Sigma^+$ and a $^2\Pi$ state are[42]

$$\langle\,^2\Pi_{1/2}Jp\mid H\mid\,^2\Sigma_{1/2}^+NJ\rangle = \langle\Pi\mid\tfrac{1}{2}AL_+\mid\Sigma\rangle$$
$$+\langle\Pi\mid BL_+\mid\Sigma\rangle[1+(-1)^{J+N+1/2}(J+\tfrac{1}{2})]\quad\text{(A1)}$$

and

$$\langle\,^2\Pi_{3/2}Jp\mid H\mid\,^2\Sigma_{1/2}^+NJ\rangle = \langle\Pi\mid BL_+\mid\Sigma\rangle$$
$$\times[(J-\tfrac{1}{2})(J+\tfrac{3}{2})]^{1/2},\quad\text{(A2)}$$

where the parity p of the Π level is $(-1)^N$.

The electronic matrix elements have been obtained in several microwave and ESR studies on the OH

ground state.[3] We use the recent values of Clough, Curran, and Thrush, namely, for $v''=0$ of OH

$$\langle \Pi \mid BL_+ \mid \Sigma \rangle = 25.146 \text{ cm}^{-1} \qquad (A3)$$

and

$$\langle \Pi \mid \tfrac{1}{2}AL_+ \mid \Sigma \rangle = -76.32 \text{ cm}^{-1}. \qquad (A4)$$

The value of $\langle \Pi \mid BL_+ \mid \Sigma \rangle$ for OD may be obtained from (A3) using the isotope rule; the value of $\langle \Pi \mid \tfrac{1}{2}AL_+ \mid \Sigma \rangle$ for OD is the same as in OH. The off diagonal spin–orbit contribution to the value of the spin–rotation constant γ is given by

$$\gamma = 4\langle \Pi \mid \tfrac{1}{2}AL_+ \mid \Sigma \rangle \langle \Pi \mid BL_+ \mid \Sigma \rangle / (E_\Pi - E_\Sigma)_{\text{eff}}. \qquad (A5)$$

Other contributions to γ have been found to be much less in general.[43] In Eq. (A5) $(E_\Pi - E_\Sigma)_{\text{eff}}$ may be taken to have the same value but opposite sign of $(E_\Sigma - E_\Pi)_{\text{eff}}$ for the $v=0$ $^2\Pi$ state because the Franck–Condon factor for the (0, 0) band is so close to unity. Using (A3), (A4), and $(E_\Pi - E_\Sigma)_{\text{eff}} = -32\ 665$ cm^{-1}, we obtain from Eq. (A5) the value $\gamma(v=0) = 0.2350$ cm^{-1}. This should be compared with the experimental value[1] of $\gamma = 0.2244$ cm^{-1}. The difference is less than 5%. Within 15% uncertainties in $\langle \Pi \mid \tfrac{1}{2}AL_+ \mid \Sigma \rangle$ and $\langle \Pi \mid BL_+ \mid \Sigma \rangle$, we accept the above model and the above values for purposes of computing perturbation corrections to the Zeeman effect.

The perturbed $^2\Sigma^+$ wavefunction will be, to first order,

$$\mid {}^2\Sigma^+ NJ \rangle_1 = \mid {}^2\Sigma^+ NJ \rangle + C(\tfrac{1}{2}; Jp) \mid {}^2\Pi_{1/2} Jp \rangle$$
$$+ C(\tfrac{3}{2}; Jp) \mid {}^2\Pi_{3/2} Jp \rangle, \qquad (A6)$$

where

$$C(\Omega; Jp) = \langle {}^2\Sigma^+ NJ \mid H \mid {}^2\Pi_\Omega Jp \rangle / (E_\Sigma - E_\Pi)_{\text{eff}} \qquad (A7)$$

and may be evaluated from Eqs. (A1)–(A4). All hyperfine components of a given NJ level contain $^2\Pi$ admixture of the same fraction. Therefore the correction terms may be applied to the part of Eq. (13) that is independent of nuclear spin. For the pure $^2\Sigma^+$ terms, this gives the usual $^2\Sigma^+$ g values for $I=0$. Thus the first-order Zeeman effect may be written

$$_1\langle {}^2\Sigma^+ JN \mid H_z \mid {}^2\Sigma^+ JN \rangle_1 = \langle {}^2\Sigma^+ JN \mid H_z \mid {}^2\Sigma^+ JN \rangle$$
$$+ 2C(\tfrac{1}{2}; Jp) \langle {}^2\Sigma^+ JN \mid H_z \mid {}^2\Pi_{1/2} Jp \rangle$$
$$+ 2C(\tfrac{3}{2}, Jp) \langle {}^2\Sigma^+ JN \mid H_z \mid {}^2\Pi_{3/2} Jp \rangle$$
$$= \pm [M\mu_0 H / (N + \tfrac{1}{2})][1 + \delta] \qquad (A8)$$

where the $\pm$ sign refers to $J = N \pm \tfrac{1}{2}$. The off-diagonal Zeeman matrix elements are evaluated as in the manner indicated by Freed[44] but with our sign convention. We use for the reduced element $\langle \Sigma \mid L_+ \mid \Pi \rangle$ the value 1.34 which is taken from Clough et al.[3] Within our experimental uncertainties, the correction to g_F caused by (A, X) mixing may be neglected.

In order to compute the effect of the (A, X) mixing

on the optical transition moment, we need to develop the perturbed $^2\Pi$ wavefunctions. For a given level Jpi, where $i = 1$ or 2 refers to the F_1 or F_2 component of the $^2\Pi$ state, the wavefunction may be written in terms of the case (a) parity basis set as[42]

$$\mid {}^2\Pi Jpi \rangle = u(\tfrac{1}{2}; Jpi) \mid {}^2\Pi_{1/2} Jp \rangle + u(\tfrac{3}{2}; Jpi) \mid {}^2\Pi_{3/2} Jp \rangle, \qquad (A9)$$

where the u's are the elements of a unitary transformation that diagonalizes the $^2\Pi$ Hamiltonian. The (A, X) mixing modifies (A9) to read to first order

$$_1\langle {}^2\Pi Jpi \mid = \sum_\Omega u(\Omega; Jpi) [\langle {}^2\Pi_\Omega Jp \mid$$
$$- C(\Omega; Jp) \langle {}^2\Sigma^+ JN \mid]. \qquad (A10)$$

With Eqs. (A6) and (A10) the optical transition moment between the levels $^2\Pi J_1 p_1 i$ and $^2\Sigma^+ N_2 J_2$ becomes, to first order,

$$\mid {}_1\langle {}^2\Pi J_1 p_1 i \mid \boldsymbol{\mu} \cdot \boldsymbol{\varepsilon} \mid {}^2\Sigma^+ N_2 J_2 \rangle_1 \mid {}^2$$
$$= \mid \sum_\Omega u(\Omega; J_1 p_1 i) \{ \langle {}^2\Pi_\Omega Jp \mid \boldsymbol{\mu} \cdot \boldsymbol{\varepsilon} \mid {}^2\Sigma^+ N_2 J_2 \rangle$$
$$+ C(\Omega; J_2 p_2) \langle {}^2\Pi_\Omega J_1 p_1 \mid \boldsymbol{\mu} \cdot \boldsymbol{\varepsilon} \mid {}^2\Pi_\Omega J_2 p_2 \rangle$$
$$- C(\Omega; J_1 p_1) \langle {}^2\Sigma^+ J_1 N_1 \mid \boldsymbol{\mu} \cdot \boldsymbol{\varepsilon} \mid {}^2\Sigma^+ J_2 N_2 \rangle \} \mid {}^2, \qquad (A11)$$

where in deriving Eq. (A11) we use the fact that $\langle {}^2\Pi_{1/2} \mid \boldsymbol{\mu} \cdot \boldsymbol{\varepsilon} \mid {}^2\Pi_{3/2} \rangle$ vanishes for pure Hund's case (a) coupling [See Eq. (18)].

The correction terms to the $A-X$ transition moment involve the weighted difference between the matrix elements

$$\langle {}^2\Pi_\Omega J_1 p_1 \mid \boldsymbol{\mu} \cdot \boldsymbol{\varepsilon} \mid {}^2\Pi_\Omega J_2 p_2 \rangle$$

and

$$\langle {}^2\Sigma^+ J_1 N_1 \mid \boldsymbol{\mu} \cdot \boldsymbol{\varepsilon} \mid {}^2\Sigma^+ J_2 N_2 \rangle.$$

The matrix elements are related to the square root of a rotational line strength for a $^2\Pi$–$^2\Pi$ or a $^2\Sigma$–$^2\Sigma$ transition times the dipole moment of the $^2\Pi$ or $^2\Sigma$ state, respectively. Equation (A11) shows that the lifetime correction is determined by a complicated sum of several terms for each branch. We have performed this evaluation using the experimental dipole moments, which are known from ab initio calculation to have the same polarity. We find that there is a shift in the radiative lifetime of 4.8 ± 1.3 nsec for $J = N \pm \tfrac{1}{2}$ at $N = 2$, and only 3.8 ± 1.6 nsec for $J = N \pm \tfrac{1}{2}$ at $N = 10$. The sign of this correction depends on the choice of relative phase of the A and X state dipole moments with respect to the $A-X$ dipole transition moment. Because of extensive cancellation the variation of τ of f_{00} with N and J caused by (A, X) mixing is quite small. In the absence of another mechanism, rotational-electronic mixing does not appear to cancel the variation caused by centrifugal distortion.

APPENDIX B: DERIVATION OF DOUBLE RESONANCE SIGNAL INTENSITY FROM A DENSITY MATRIX EXPANSION IN MULTIPOLE MOMENTS

Equation (32) has been given without proof in the work of Happer and Saloman.[23] However, because of its importance to double resonance in molecules we present a brief derivation here.

Equation (32) may be obtained by following a derivation similar to that of Carver and Partridge.[22] In this case, ρ^0 is defined by Eq. (24) as an expansion in multipole moments, and the transformation to the rotating frame also is performed in the LM representation. Alternatively, we will show the equivalence of Eq. (32) with Eq. (19).

A spherical irreducible tensor operator transforms under rotation as

$$RT(L, M)R^{-1}= \sum_{M'} D_{M'M}{}^{L}T(L, M). \qquad (B1)$$

Equation (B1) may be rewritten with explicit matrix indices as

$$\sum_{m,m'} d_{nm}{}^{F}(\theta)T(L, M')_{mm'}d_{m'n'}{}^{F}(-\theta)$$
$$= \sum_{M'} d_{M'M}{}^{L}(\theta)T(L, M')_{nn'}, \qquad (B2)$$

where we have specialized R to be the transformation in the rotating frame which rotates the axis of quantization from $\mathbf{H}_0$ to $\mathbf{H}_{\mathrm{eff}}$ and where $T(L, M)_{mm'}$ vanishes unless $m'=m+M$. With Eq. (26) the resonance equation (19) becomes

$$\rho_{mm}=W \sum_{L,m_0,n,n'} \rho(L)E_i(L, O) \frac{d_{mn}{}^{F}(\theta)d_{nm_0}{}^{F}(-\theta)T(L, O)_{m_0m_0}d_{m_0n'}{}^{,F}(\theta)d_{n'm}{}^{F}(-\theta)}{\Gamma+ip(n-n')}$$

$$=W \sum_{L,M',n,n'} \rho(L)E_i(L, O) \frac{d_{M'O}{}^{L}(-\theta)d_{mn}{}^{F}(\theta)T(L, M')_{nn'}d_{n'm}{}^{F}(-\theta)}{\Gamma+i(n-n')p}$$

$$=W \sum_{L,M'} \rho(L)E_i(L, O) \frac{d_{M'O}{}^{L}(-\theta)d_{OM'}{}^{L}(\theta)T(L, O)_{mm}}{\Gamma-iM'p} \qquad (B3)$$

Using Eqs. (14), (25), and (29) we obtain the form

$$I=W \sum_{L} \rho(L)\mathfrak{M}(L)E_i(L, O)E_f(L, O) \sum_{M'} [d_{OM'}{}^{L}(\theta)d_{M'O}{}^{L}(-\theta)/(\Gamma-iM'p)]. \qquad (B4)$$

The generalization of this derivation to include $m \neq m'$ and $m_0 \neq m_0'$, as would be required for the modulated fluorescence terms, is straightforward.

To obtain the convenient expression Eq. (33), we substitute in (B4) explicit algebraic expressions[45] for $d_{OM'}{}^{2}(\theta)$. The summation in (A4) for the $L=2$ term becomes

$$\sum_{M'} \frac{d_{OM'}{}^{2}(\theta)d_{M'O}{}^{2}(-\theta)}{\Gamma-iM'p} = \frac{3\Gamma}{4} \frac{\sin^4\theta}{\Gamma^2+4p^2} + \frac{3\Gamma \sin^2\theta \cos^2\theta}{\Gamma^2+p^2} + \frac{(3 \cos^2\theta-1)^2}{4\Gamma}. \qquad (B5)$$

Using the identity

$$\cos\theta= (\omega-\omega_0)/[(\omega-\omega_0)^2+\omega_1^2] \qquad (B6)$$

we obtain

$$I= W\Gamma^{-1} [\rho(O)\mathfrak{M}(O)E_i(O, O)E_f(O, O)+\rho(2)\mathfrak{M}(2)E_i(2, O)E_f(2, O)$$

$$\times (1- \{3\omega_1^2/[\Gamma^2+\omega_1^2+(\omega-\omega_0)^2]\} \{[\Gamma^2+\omega_1^2+4(\omega-\omega_0)^2]/[\Gamma^2+4\omega_1^2+4(\omega-\omega_0)^2]\})]. \qquad (B7)$$

The factor in boldface parentheses is equal to $2B/I_0$ in Eq. (5) of Brossel and Bitter's treatment[12] for double resonance in atomic p states. Note that at resonance where $\omega=\omega_0$, that part of (B7) responsible for the double resonance signal becomes identical with Eq. (33). Regardless of the value of F, π-polarized electric dipole excitation produces multipole elements $L=0$, $M=0$ and $L=2$, $M=0$ only. Therefore, if the matrices ρ and $\mathfrak{M}$ are expressed in a multipole expansion, Eq. (B7) will apply to double resonance in any molecular hyperfine state for which the resonance frequency is given simply by $\omega_0=g\mu_0H$.

*Present address: Bell Telephone Laboratories, Holmdel, N. J. 07733.

†Present address: Department of Physics, Fordham University, Bronx, N. Y. 10458.

‡Present address: Department of Chemistry, The University of Massachusetts at Boston, Boston, Mass. 02116.

[1] G. H. Dieke and H. M. Crosswhite, Bumblebee Rept. No. 87, John Hopkins University, 1948, republished in J. Quant.

Spectrosc. Radiat. Transfer **2**, 97 (1963). The rotational line strengths given have a number of typographical errors: Eq. (13c) should have −2 in place of −a; Eq. (13d) should have 2(a−4) in place of 2(J −4); and Eq. (13f) should have ±U in place of + U.

[2] G. C. Dousmanis, T. M. Sanders, and C. H. Townes, Phys. Rev. **100**, 1735 (1955).

[3] Microwave studies have been reported by G. Ehrenstein, C.

Townes, and M. J. Stevenson, Phys. Rev. Lett. 3, 40 (1959);
H. E. Radford, Phys. Rev. Lett. 13, 534 (1964); and R. L.
Poynter and R. A. Beaudet, Phys. Rev. Lett. 21, 305 (1968).
K. M. Evenson, J. S. Wells, and H. R. Radford, Phys. Rev.
Lett. 25, 199 (1970), have observed laser magnetic resonance
at 70 μm. EPR data are reported by H. R. Radford, Phys. Rev
Rev. 122, 114 (1961); Phys. Rev. 126, 1035 (1962); A.
Carrington and N. J. D. Lucas, Proc. R. Soc. A 314, 567
(1970); A. Churg and D. H. Levy, Astrophys. J. 162, L161
(1970); P. M. Clough, A. H. Curran, and B. A. Thrush, Proc.
R. Soc. A 323 541 (1971); and K. P. Lee, W. G. Tam, R.
Larouche, and G. A. Wooton, Can. J. Phys. 49, 2207 (1971).

[5]R. L. deZafra, A. Marshall, and H. Metcalf, Phys Rev. A
3, 1557 (1971).

[6]K. R. German and R. N. Zare, Bull. Am. Phys. Soc. 15, 82
(1970). Note the radiative lifetime should read
6.3±0.7×10^{-7} sec rather than 6.3±0.7×10^{-8} sec.

[7]E. M. Weinstock and R. N. Zare, J. Chem. Phys. 58, 4319 (1973).
(following paper).

[8]See F. P. Del Greco and F. Kaufman, Discuss. Faraday Soc.
33, 128 (1962); L. F. Phillips and H. I. Schiff, J. Chem.
Phys. 37, 1233 (1962).

[9]The R_{21} branch in the notation of Dieke and Crosswhite
corresponds to the ^RQ branch in the more common notation
of Herzberg.

[10]This assignment is based on the spectroscopic analysis of the
OD $A-X$ band system by M. Ishaq, Proc. Natl. Inst. Sci.
India A 3, 389 (1937). The Q_1 branch is the same in the
notation both of Dieke and Crosswhite and of Herzberg.
Without knowing the shape of the lamp profile we cannot
determine whether or not the $v'=0$, $N'=1$, $J'=1/2$ level is
also excited. In any event, it does not contribute to the
Hanle signal (see Ref. 11). This assignment has been
confirmed in the recent high-resolution studies of the
ultraviolet band system of OD by J. A. Coxon (private
communication), Queen Mary College, University of London.

[11]A. Gallagher and A. Lurio, Phys. Rev. Lett. 10, 25 (1963).

[12]J. Brossel and F. Bitter, Phys. Rev. 86, 308 (1952).

[13]For a discussion of Hund's coupling cases including hyperfine
interaction, see C. H. Townes and A. L. Schawlow,
Microwave Spectroscopy (McGraw-Hill, New York, 1955),
pp. 196–199.

[14]K. R. German, R. N. Zare, and D. R. Crosley, J. Chem. Phys.
54, 4039 (1971).

[15]E. A. Scarl and F. W. Dalby, Can. J. Phys. 49, 2825 (1971).

[16]M. A. A. Clyne, J. A. Coxon, and A. R. Woon Fat, "The A
$^2\Sigma^+ - X\,^2\Pi_i$ Electronic Band System of the OD Free Radical
1. Fundamental data for the 0–0 sequence, and rotational
term values for $A\,^2\Sigma^+$ and $X\,^2\Pi_i$" (unpublished).

[17]R. A. Frosch and H. M. Foley, Phys. Rev. 88, 1337 (1952).

[18]G. C. Dousmanis, Phys. Rev. 97, 967 (1955).

[19]The hfs matrix elements are taken from Eqs. (2)–(4) of H. E.
Radford, Phys. Rev. A 136, 1571 (1964).

[20] See, for example, M. Rotenberg, R. Bivins, N. Metropolis,
and J. K. Wooten, Jr., The 3-j and 6-j Symbols

(Technology, Cambridge, Mass., 1959).

[21]J. N. Dodd and G. W. Series, Proc. R. Soc. A 263, 353
(1961).

[22]T. R. Carver and R. B. Partridge, Am. J. Phys. 34, 339
(1966).

[23]W. Happer and E. B. Saloman, Phys. Rev. 160, 23 (1967).

[24]C. Cohen-Tannoudji, in Topics on Radiofrequency
Spectroscopy (Academic, New York, 1962), p. 240; J. P.
Barrat, Proc. R. Soc. A 263, 371 (1961).

[25]K. Freed, J. Chem. Phys. 45, 4214 (1966).

[26] S. J. Silvers, T. H. Bergeman, and W. A. Klemperer, J.
Chem. Phys. 52, 4385 (1970).

[27]R. W. Field and T. H. Bergeman, J. Chem. Phys. 54, 2936
(1971).

[28]S. Green (private communication), Goddard Institute for
Space Studies, New York, N. Y.

[29]T. Hollander and H. P. Broida, J. Quant. Spectrosc. Radiat.
Transfer 7, 965 (1967).

[30]Calculated from RKR potentials using the programs
documented in R. N. Zare, Rept. UCRL-10925, Lawrence
Radiation Laboratory, Berkeley, Cal., 1963.

[31]See the photoelectric intensity measurements of G. H. Dieke
as reported in R. W. Nicholls, Proc. Phys. Soc. Lond. A
69, 741 (1956).

[32]W. H. Henneker and H. E. Popkie, J. Chem. Phys. 54, 1763
(1971).

[33]J. Anketell and A. Pery-Thorne, Proc. R. Soc. A 301, 343
(1967).

[34]W. H. Smith (private communication), Princeton University
Observatory, Princeton, N. J. See also B. Elmergreen, N.
Elander, and W. H. Smith, 27th Symposium on Molecular
Structure and Spectroscopy, Columbus, Ohio, 1972,
Abstracts, p. 121,

[35]R. A. Anderson (private communication), Dept. of Physics,
University of Missouri at Rolla, Rolla, Mo. See also R. A.
Sutherland and R. A. Anderson, Bull. Am. Phys. Soc.
17, 574 (1972).

[36]J. Anketell and R. C. M. Learner, Proc. R. Soc. A 301, 355
(1967).

[37]R. C. M. Learner, Proc. R. Soc. A 269, 311 (1962).

[38]R. Jost, M. A. Maréchal, and M. Lombardi, Phys. Rev. A
5, 740 (1972).

[39]M. M. Litvak, A. L. McWharter, M. L. Meeks, and H. J.
Zeigler, Phys. Rev. Lett. 17, 821 (1966).

[40]M. M. Litvak, Interstellar Ionized Hydrogen, edited by
Yervant Terzian (Benjamin, New York, 1968), pp. 713–745.

[41]P. S. Julienne, M. Krauss, and B. Donn, Ap. J. 170, 65
(1971).

[42]J. H. Van Vleck, Phys. Rev. 33, 467 (1929).

[43]L. B. Knight, Jr., and W. Weltner, Jr., J. Chem. Phys.
54, 3875 (1971).

[44]See Eq. (11.9) of Ref. 25.

[45]D. M. Brink and G. R. Satchler, Angular Momentum
(Oxford, U. P., Oxford, England, 1962), p. 24.